Journal of Colloid and Interface Science 350 (2010) 373–376

Contents lists available at ScienceDirect

Journal of Colloid and Interface Science

www.elsevier.com/locate/jcis

Short Communication

Impact of drops on the surface of immiscible liquids

Ehsan Yakhshi-Tafti, Hyoung J. Cho, Ranganathan Kumar *

Department of Mechanical, Material and Aerospace Engineering, 4000 Central Florida Blvd., Orlando, FL 32816, USA

ARTICLE INFO

Article history:
Received 6 April 2010
Accepted 12 June 2010
Available online 19 June 2010

Keywords:
Drop impact on immiscible liquids
Free surface
Drop shape

ABSTRACT

Impact of drops on the surface of an immiscible liquid is studied. We show that in addition to the commonly-observed lens structure at the air–liquid interface, drops released from critical heights above the target liquid can sustain the impact and at the end maintain a spherical ball-shape configuration above the surface despite undergoing large deformation. The existence of this metastable state of the drop above the free surface and its transition into the more stable submerged lens configuration at the air–liquid interface is investigated. The initial impact which induces the degree of submergence is critically related to the two distinct life paths of drops impinging upon a liquid surface.

Impingement of drops on solid and liquid surfaces has been studied extensively. Such studies were motivated by applied purposes such as spray cooling [1,2], inkjet printing [3], soil erosion due to rain [4] and understanding and quantifying rainfall [5] or for fundamental understanding of the underlying physics, which often leads to complex mathematical description of the phenomenon [6–10]. A thorough review on the topic has been carried out by Rein [11] and Yarin [12].

Drops impinging on the surface of a liquid can splash [7,13], coalesce with or bounce off the surface [11] depending on various factors including impact velocity of the drop, the depth of the target liquid and the physical properties of the fluids. Typically, when a drop collides with the liquid surface at a relatively high speed, a crater is formed. Due to instability of the rising liquid sheet on the rim, smaller jets are ejected and the resulting structure resembles a crown; these jets further breakup into spray droplets. As the walls of the crater rim subside, the receding flow towards the center shoots up in form of a column of fluid which also breaks up and secondary drops are ejected in the vertical direction [6,8,12]. In addition to impact velocity, experimental results show the dependency of splash, deposition and crown formation of impinging drops on liquid films on fluid viscosity and film thickness [14,15]. It has been found that in the limit of extremely thin target films, the critical splashing following impact of drops is insensitive to the film thickness for given underlying solid surfaces [16].

Generally, drops impinging on the surface of self-similar liquids eventually coalesce with the target pool, or form a lens-shaped structure on the free surface of immiscible liquids. However, spherical ball-shaped drops have also been observed that exist at the air–liquid interface. Such isolated drops on the surface of similar liquids have been attributed mainly to the existence of a cushion of trapped air which serves as a lubricating film, preventing it from coalescing with the bulk liquid [17,18]. This effect is better seen when the target liquid pool is set to vibrate in the normal direction [19,20]. A similar bouncing/anti wetting effect is observed for drops impinging upon super-hydrophobic solid substrates [21].

In this report, we show that drops impinging upon the surface of an immiscible liquid can retain a metastable spherical configuration above the surface following the impact without collapsing into the target liquid in form of a partially-submerged lens-shape. This configuration is commonly-observed for drops resting at the interface of other immiscible liquids. We show that such spherical drops can retain their shape unless the system is disturbed which causes them to break down into partially-submerged lens structures. Precision dispensing needles were used to release drops of deionized water onto the surface of fluorocarbon liquid (FC-43, 3 M). Drop impact was recorded by a high speed camera at a rate of 2000 frames per second.

Fig. 1 shows the time progression of the impact and one cycle of drop oscillation on the surface. It is seen that both the target liquid and the drop undergo large deformations during the impact; however, the drop is able to maintain its spheroid structural integrity after the impact. The deformations are similar to the morphologies reported for drops impacting upon soft solids [22] but they are not large enough to result in the splitting of the original drop. The amplitude of deformation dies out quickly within the first few oscillation cycles (Video 1 in supporting information).

Fig. 2a provides the range of the critical release-heights for which various size drops are able to sustain the impact and keep a spherical shape while the underlying liquid sheet stretches to accommodate the impact. The gray area on the graph represents a collection of release-heights for which drops rebound on the surface and form a

* Corresponding author.
E-mail address: rnkumar@mail.ucf.edu (R. Kumar).

0021-9797/$ - see front matter © 2010 Elsevier Inc. All rights reserved.
doi:10.1016/j.jcis.2010.06.029

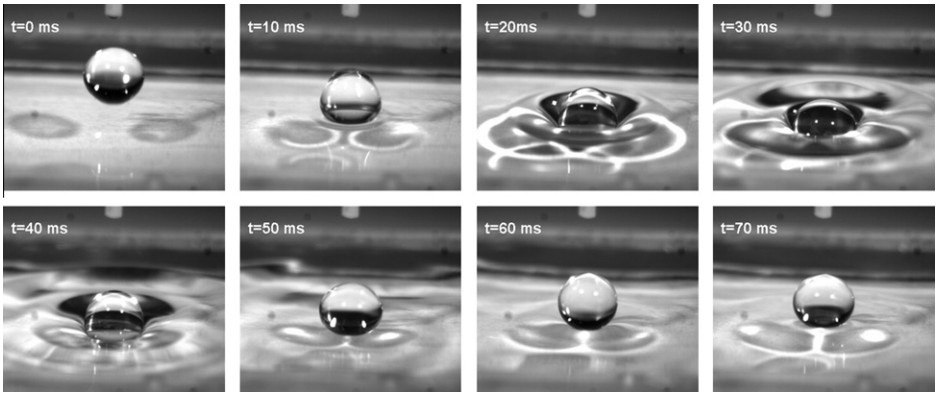

Fig. 1. Impact and oscillation of a drop of water on the surface of fluorocarbon liquid FC-43 (Video 1 in supporting information).

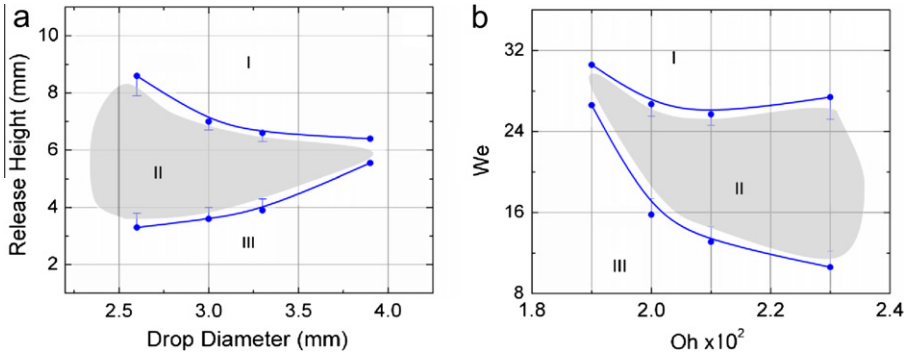

Fig. 2. (a) Release-height as a function of drop diameter and (b) We as a function of *Oh*. (I) Region in which drops collapse into lens-shaped drops. (II) Region in which drops assume a spherical ball-shape above the surface. (III) Region in which the drops bridge the gap between the dispensing tip and the liquid interface where free falling pendant drops cannot be formed.

spherical structure above the interface. Similar spherical drops on liquid surfaces have been shown by isolating the two fluids for example by coating the exterior of the drops by super-hydrophobic powders [23]. The critical release-height for drops released from a 27G needle ranges from about 1.5–3 times the drop diameter and gets narrower for smaller gauged needles (larger drops). A cubic relationship was found between the diameter of the needle tip and the pendant drops that were released due to their own weight.

Weber number ($We = \rho U^2 D/\sigma$), Ohnesorge number ($Oh = \mu/\sqrt{\rho\sigma D}$), normalized film thickness ($t^* = t/D$) and the Bond number ($Bo = \rho g h^2/\sigma$) are commonly used in analysis of such systems (σ is the target liquid's surface tension, ρ the density of the drop, D the drop diameter and U is the impact speed which is a function of release-height as $U = \sqrt{2gH}$. The Ohnesorge number relates the viscous forces to inertial and surface tension forces, Weber number is used for evaluating the relative importance of inertia and surface tension and the Bond number compares the gravitational force to surface tension effects. Using the physical properties of water and fluorocarbon FC-43, the conditions of the experiment are characterized by $Oh \approx 0.02$, $We \approx 20$ ($Bo \approx 10$) for $t^* \approx 4$. It is seen that as the drops get larger, the critical height range for successful rebound becomes more limited. Critical parameters for which, free falling drops are able to sustain the impact and retain a spherical ball-shape at the interface range over the gray region (area II) shown in Fig. 2. Larger drops and those released from higher than critical heights were found to collapse immediately into a lens-shaped structure in the process of impact as commonly-observed (area I). The lower bound of release-heights in experiments resulted from the minimum distance between the needle tip and the interface such that pendant drops could be formed; for shorter distances drops formed a bridge between the tip and the target liquid and did not get released into a free fall (area III).

The spherical drops can remain intact on the surface; however, they are unstable and have a tendency to collapse into the submerged configuration if there are any perturbations or vibrations. Fig. 3 shows the breakup and transformation of a spherical drop into a lens structure at the air–liquid interface (Video 2 in supporting information); a process which completes in less than a tenth of a second. It is seen that the drop undergoes rapid and asymmetric deformations from the bottom and the sides until it eventually settles into a symmetric shape partially-submerged in the target liquid. Static conditions for the drop can be determined by carrying out a force analysis or by evaluating the total energy of the system.

A balance of forces in the vertical direction can be used to find the equilibrium static state. Similarly, extrema of the system's energy (surface energy and work of the external forces acting on the system) can also provide equilibrium states (drop configuration at the interface) that determine the stability of a given static configuration [24]. Considering Fig. 4, there are three forces that act on the drop in the vertical direction [25]:

Drop weight: $F_G = 4/3\pi g \rho_w r^3$.
Surface tension force: $F_S = 2\pi\sigma_f r \sin(\varphi)\sin(\varphi + \theta)$ exerted by the drop on the target liquid.
Buoyancy force: $F_B = \pi g \rho_f [h_0 r^2 \sin^2(\varphi) + \pi g r^3 \sin^2(\varphi)\cos(\varphi) + 2/3 r^3(\cos^3(\varphi) - 1)]$ found by integrating the vertical component of the hydrostatic pressure force around the drop. In these expressions, r is the equivalent radius of a sphere that would give the drop volume, $\rho_f = 1880\ \mathrm{kg/m^3}$, $\rho_w = 998\ \mathrm{kg/m^3}$ are the density of the base liquid and the water drop and the density

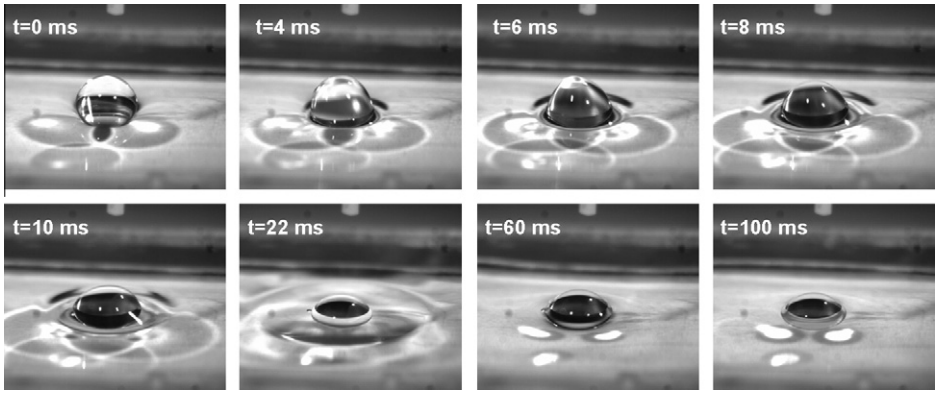

Fig. 3. Collapse of a spherical drop into partially-submerged lens configuration (Video 2 in supporting information).

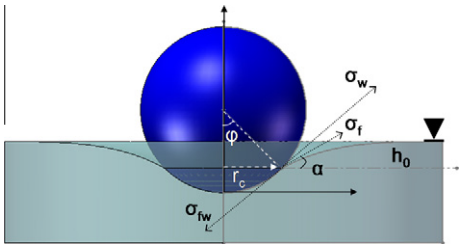

Fig. 4. Schematic of a spherical drop resting at the liquid–air interface.

of the surrounding air is neglected. σ_f = 16 dyne/cm, σ_w = 71 dyne/cm and σ_{fw} = 52 dyne/cm are the surface (interfacial) tensions of the target liquid (FC-43)–air, drop (water)–air and drop–target liquid pairs respectively, measured by the pendant drop method.

The angle φ represents the extent of submergence of the drop in the target liquid; by varying φ from 0 (above the surface an touching) to 180° (fully submerged), the net force (normalized by $r\sigma_f$) acting on the drop can be plotted as a function of φ. The angle, φ_s, corresponding to the zero-sum of forces shows the equilibrium static condition. It is noted that in order to evaluate the buoyancy force, the capillary rise (fall) of the target liquid on the drop, h_0, is needed (h_0, is measured from the free surface to three phase contact line). For the case of spherical drops, h_0 is not readily available [26] and should be found by numerically solving the Young–Laplace equation that gives the free surface profile in the vicinity of the contact line:

$$\left[\frac{d^2z/dx^2}{[1+(dz/dx)^2]^{3/2}}+\frac{dz/dx}{x[1+(dz/dx)^2]^{1/2}}\right]-\frac{\rho_f g z}{\sigma_f}=0$$

The governing equation for the capillary profile was numerically solved with the boundary conditions: $dz/dx = \tan(\alpha)$ at $x = r_c$ (r_c contact line radius) and $dz/dx = 0$ as $x \to \infty$ (we found ∞ to be around three times the drop diameter by extending the solution for larger x). $\alpha = \theta + \varphi - \pi$, and θ is the equilibrium contact angle and is measured counterclock wise from σ_{fw} to σf. In current experiments the equilibrium contact angle was found to be $\theta_e = 15° \pm 3°$ (error is due to the misalignment of the imaging camera with the horizontal line).

As seen in Fig. 5, the net vertical force becomes zero at $\varphi \approx 144°$ which denotes the partially-submerged configuration as the static equilibrium condition. This angle is in good agreement with the observed extent of immersion of the drop in the lens configuration from imaging, $\varphi_s = 140°$ (Fig. 6b).

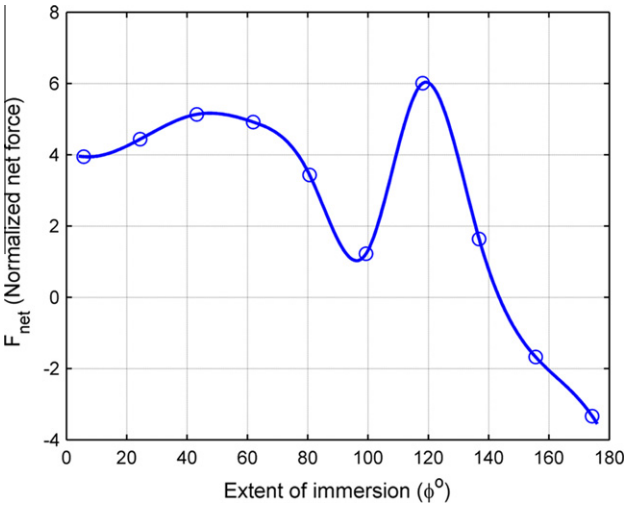

Fig. 5. Net vertical force as a function of the extent of drop submergence in the target liquid.

It is noted that the force analysis is performed by approximating the drop to a spherical volume. The exact shape of a drop residing at the interface of two fluids has been described in detail [27] as the drop breaks down and submerges in the base liquid.

While we observe two distinct static configurations for the drops at the interface, only the lens configuration is predicted by the force balance model (ΣF plotted against φ has a single zero, Fig. 5). The net force (sinking) has a negative slope when passing the equilibrium, which physically translates to the following: the sinking force would decrease (changes signs and becomes upward) if the drop were to be further immersed in the base liquid and since it would not accelerate against the direction of gravity, the drop would eventually rest at this state. The force balance provides only the *equilibrium* static states because the thermodynamic equilibrium contact angle θ_e is used; in addition it is assumed that the Young Laplace equation is satisfied at the drop–liquid interface profile. Static conditions other than the equilibrium, for example the spherical configuration observed here, are known as *mechanically enforced stationary* states [24,28] that are achieved with the aid of some external agents present in the system that compensate for the non-zero net *equilibrium* forces. The spherical drop in our case is predicted not to be at static equilibrium due to the equilibrium force imbalance; however it does exist in a static state in our experiments. Existence of a fine interfacial air film has been confirmed for non-coalescent drops impinging on the surface of self-similar liquid films [17,18]. Though this could not be confirmed, it is likely that an extremely thin cushion of air balances the net

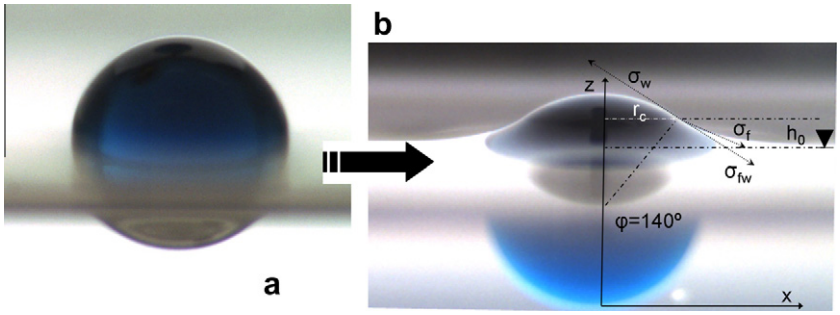

Fig. 6. Spherical drop (a) converts into the stable partially-submerged lens-shape configuration (b).

vertical force and allows the existence of the isolated spherical drop on the free surface in current experiments. The thickness of such an air film is estimated to be larger than the Van der Waals attraction (~10 nm).

In summary, we studied the impact of a drop onto the surface of an immiscible liquid and demonstrated the possibility of creating isolated spherical drops above a liquid interface without external stimuli such as induced vibration on the surface [21] or hydrophobic coatings [23] or temperature difference between drop and target liquid [29]. Released from a controlled height and depending on their size, liquid drops colliding on the surface of immiscible liquids can sustain the impact and maintain their spherical integrity over the air–liquid interface. The target liquid deforms similar to an elastic membrane and causes the drop to rebound and oscillate on the surface. The impact and the oscillation process are completed in less than 70 ms due to relatively large viscous damping. Spherical drops collapse and transform into the more stable and commonly-observed partially-submerged lens-shaped configuration if any perturbations exist. The equilibrium force balance predicts only the lens-shape as the stable configuration and the extent of submergence found is in good agreement with our observations from imaging. Liquid drops resting on the free surfaces of inert liquid platforms exhibit interesting features and show promise for various applications such as material transport vehicles for lab on chips [30].

Appendix A. Supplementary material

Supplementary data associated with this article can be found, in the online version, at doi:10.1016/j.jcis.2010.06.029.

References

[1] J. Kim, Int. J. Heat Fluid Flow 28 (2007) 753.
[2] A.N. Lembach, H.-B. Tan, I.V. Roisman, T. Gambaryan-Roisman, Y. Zhang, C. Tropea, A.L. Yarin, Langmuir (2010).
[3] D.B. van Dam, C. Le Clerc, Phys. Fluids 16 (2004) 3403.
[4] A.J. Moss, P. Green, Aust. J. Soil Res. 21 (1983) 257.
[5] E. Villermaux, B. Bossa, Nat. Phys. 5 (2009) 697.
[6] F.H. Harlow, J.P. Shannon, Science 157 (1967) 547.
[7] P.V. Hobbs, A.J. Kezweeny, Science 155 (1967) 1112.
[8] W.C. Macklin, P.V. Hobbs, Science 166 (1969) 107.
[9] L. Xu, W.W. Zhang, S.R. Nagel, Phys. Rev. Lett. 94 (2005) 184505.
[10] L. Xu, L. Barcos, S.R. Nagel, Phys. Rev. E 76 (2007) 066311.
[11] M. Rein, Fluid Dyn. Res. (1993) 61.
[12] A.L. Yarin, Annu. Rev. Fluid Mech. 38 (2006) 159.
[13] P.V. Hobbs, T. Osheroff, Science 158 (1967) 1184.
[14] G. Cossali, A. Coghe, M. Marengo, Exp. Fluids 22 (1997) 463.
[15] R. Rioboo, C. Bauthier, J. Conti, M. Voué, J. De Coninck, Exp. Fluids 35 (2003) 648.
[16] A.-B. Wang, C.-C. Chen, Phys. Fluids 12 (2000) 2155.
[17] S.T. Thoroddsen, T.G. Etoh, K. Takehara, J. Fluid Mech. 478 (2003) 125.
[18] M.S. Khan, D. Kannangara, W. Shen, G. Garnier, Langmuir 24 (2008) 3199.
[19] T. Gilet, N. Vandewalle, S. Dorbolo, Phys. Rev. E 76 (2007) 035302.
[20] Y. Couder, E. Fort, C.H. Gautier, A. Boudaoud, Phys. Rev. Lett. 94 (2005) 177801.
[21] D. Richard, D. Quere, EPL (Europhys. Lett.) (2000) 769.
[22] R. Rioboo, M. Voue, H. Adao, J. Conti, A. Vaillant, D. Seveno, J. De Coninck, Langmuir (2009).
[23] P. Aussillous, D. Quere, Proc. R. Soc. A: Math., Phys. Eng. Sci. 462 (2006) 973.
[24] A.V. Rapacchietta, A.W. Neumann, S.N. Omenyi, J. Colloid Interface Sci. 59 (1977) 541.
[25] A.V. Rapacchietta, A.W. Neumann, J. Colloid Interface Sci. 59 (1977) 555.
[26] C. Huh, L.E. Scriven, J. Colloid Interface Sci. 30 (1969) 323.
[27] E.F. Greco, R.O. Grigoriev, Phys. Fluids 21 (2009) 042105.
[28] A.W. Neumann, R.J. Good, J. Colloid Interface Sci. 38 (1972) 341.
[29] R. Savino, D. Paterna, M. Lappa, J. Fluid Mech. 479 (2003) 307.
[30] V. Srinivasan, V.K. Pamula, R.B. Fair, Anal. Chim. Acta 507 (2004) 145.